Int. J. Nano Dimens., 11 (4): 355-363, Autumn 2020

ORIGINAL ARTICLE

Enhanced structural, optical and antibacterial activities of Zn_2SnO_4 nanorods synthesized by Microwave assisted method

*Arumugam Pandimurugan, Krishnasamy Sankaranarayanan**

Department of Physics, Alagappa University, Karaikudi-630 004, Tamil Nadu, India.

Received 06 May 2020, ; revised 17 June 2020; accepted 28 June 2020; available online 17 July 2020

Abstract

In this research, Zn_2SnO_4 nanorods were prepared and structural properties of the nanorods were characterized, developing of wide-range of the optical behavior of Zn_2SnO_4 nanorods and the antibacterial activity was also investigated using a microwave-assisted method. A zinc stannate (Zn_2SnO_4) nanorod was synthesized via facile microwave-assisted method using ammonia with cubic spinel structure. The crystallography and optical properties were studied using X-ray diffraction and photoluminescence spectroscopy. The morphology of the nanoparticles was observed using field emission scanning electron microscopy. The antibacterial effect of Zn_2SnO_4 nanoparticles tested against Gram-positive and Gram-negative pathogenic bacteria was investigated. The Zn_2SnO_4 nanorods showed the excellent antibacterial activity, the inhibition zone indicates the biocidal action of Zn_2SnO_4 nanorods. Here, we concluded that these materials were used as a bactericidal agent to prevent and control the spread and persistence of infectious diseases.

Keywords: *Antibacterial Activity; Nanoparticles; Nanoarchitectonics; PL; Zinc Stannate.*

How to cite this article

andimurugan A., Sankaranarayanan K. Enhanced structural, optical and antibacterial activities of Zn_2SnO_4 nanorods synthesized by Microwave assisted method. Int. J. Nano Dimens., 2020; 11 (4): 355-363.

INTRODUCTION

Zn_2SnO_4 an inverse structure of AB_2O_4 compound (space group Fd3m), has fascinated and unique properties rendering it suitable for a wide variety of applications such as chemical sensors, photoelectrical devices, transparent conducting electrodes, functional coatings and photocatalysts [1- 3]. And also, as an important transparent semiconductor with a wide bandgap of 3.6 eV, Zn_2SnO_4 is known to have high chemical sensitivity, high electrical conductivity, and low visible absorption [4]. To realize the universal application of nanomaterials, the key point is to devise simple and efficient methods for their preparation on a large scale at a low cost. Various methods have been employed to produce Zn_2SnO_4 nanostructures such as mechanochemical synthesis, thermal evaporation method by heating metal or metal oxide powder at high temperatures, simple co-precipitation method, and hydrothermal synthesis [5-7].

Metal oxide nanoparticles (NPs) are the most widely used antimicrobial agent in the food industry applications [8]. Zn_2SnO_4 NPs display biocidal activity against a broad range of Gram-positive and Gram-negative microorganisms [9]. The antimicrobial activity of Zn_2SnO_4 NPs is mainly based on the following mechanisms: (a) release of Zn^{2+}/Sn^{2+} ions which bind to electron donor groups in molecules containing sulfur, oxygen or nitrogen, (b) disruption of DNA replication and (c) oxidative stress through the catalysis of reactive oxygen species (ROS) formation [10]. ROS contains the most reactive hydroxyl radical (OH), the less toxic superoxide anion radical (˙O2-), and hydrogen peroxide with a weaker oxidizer (H_2O_2). This can damage DNA, cell membranes, etc., leading to cell death [11].

* Corresponding Author Email:
alufunctionalmaterialslab@yahoo.com

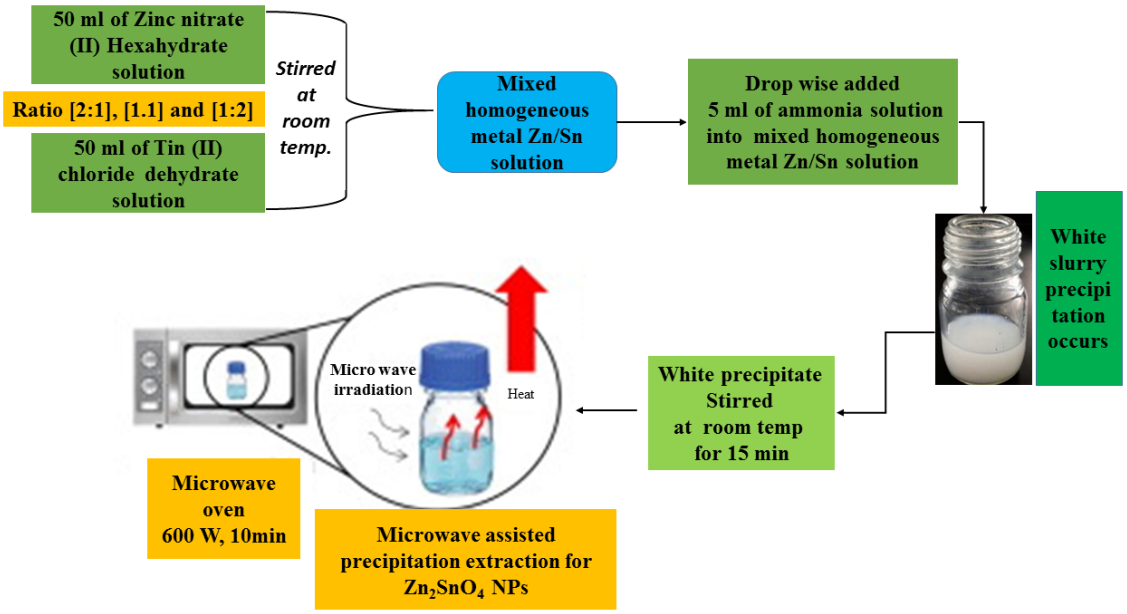

Fig. 1. Schematic diagram for the formation of Zn_2SnO_4 nanorods.

Samreen Fatema *et al.*, [12] had investigated Saraca Asoka leave extracts used successfully for the synthesis of silver nanoparticles. Their results showed anti-bacterial activities against gram-positive bacteria. Leila Kafi-Ahmadi *et al.*, [13] had examined the influence of reaction parameters on crystal phase growth and optical properties of ultrasonic-assisted Hydro-and solvothermal synthesized sub-micrometer-sized CdS spheres. Navid Assi *et al.*, [14] had studied the synthesis of ZnO-nanoparticles by microwave-assisted sol-gel method and its role in photocatalytic degradation of food dye Tartrazine. Rejani *et al.*, [15] had reported that structural, optical, and dielectric studies in ZnO nanorods by the microwave-assisted method.

In the present work, Zn_2SnO_4 nanorods were prepared by a microwave-assisted method. The structural properties of the nanorods were characterized in detail. Besides, further development of a wide range of the optical behavior of Zn_2SnO_4 nanorods and the antibacterial activity was also investigated.

EXPERIMENTAL METHODS

Synthesis

The subsequent high purity chemicals such as Zinc (II) nitrate, Tin (II) chloride dihydrate and ammonia solution were used as precursors without further purification.

Zn_2SnO_4 nanoparticle was prepared in different ratios of Zn and Sn (2 : 1, 1 : 1, and 1 : 2 named as P1, P2, and P3 respectively) by Microwave-assisted precipitation method. Zinc (II) nitrate and Tin (II) chloride aqueous solutions (50 mL) of the appropriate amount was prepared and stirred together for 1 h 20 min to get a homogeneous mixture. Then Ammonia solution was added to get a white precipitate and stirred at room temperature for 15 minutes. The product solution was transferred to a polypropylene capped autoclave bottle and the solution was irradiated by a microwave oven with a power of 600 W for 10 min. After irradiation, the solution was allowed to cool down naturally to room temperature. The precipitation was collected and washed numerous times with double distilled water and ethanol. Then the precipitate was dried at 120 °C or 12 h at the atmospheric condition and annealed at 800 °C for 5 hours to obtain Zn_2SnO_4 nanorods. The schematic diagram for the preparation of Zn_2SnO_4 nanorods is shown in Fig.1.

Antibacterial assays

The antibacterial activity of microwave assisted Zn_2SnO_4 nanorods was tested against *Streptococcus pneumoniae, Escherichia coli, Klebsiella pneumoniae and Shigella dysenteriae bacterial strain* were carried out in agar by well diffusion method. These four strains were

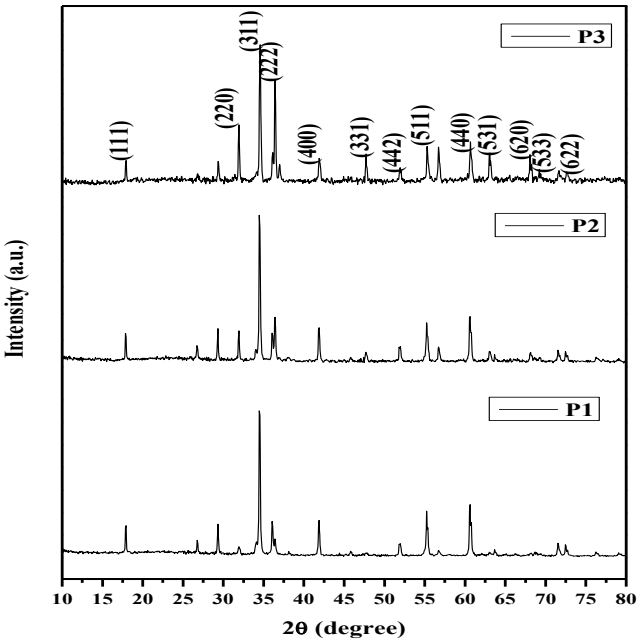

Fig. 2. X-ray diffraction patterns of Zn_2SnO_4 nanorods (P1, P2, P3).

collected from Microbiology department of Alagappa University, Karaikudi, Tamilnadu. The antibacterial activity was tested at a concentration of 1 and 1.5 mg/ml of the Zn_2SnO_4nanorods dispersed in dimethylsulphoxide (DMSO). Zn_2SnO_4 nanorods -impregnated discs (30 µl) were placed on agar plates and incubated at 37°C for 24 hours. Pure DMSO (30 µl) was used as a negative control. The zone of inhibition levels (mm) was measured subsequently after 24 h at 37 °C. For positive control, standard antibiotic Amoxicillin (30 µg disc) was used.

Characterization techniques

The structural properties of Zn_2SnO_4 nanorod was investigated from the X-Ray diffraction patterns obtained using X'PERT PRO Panalytical Diffractometer. The morphology of Zn_2SnO_4 nanorods was examined by FESEM (Carl Zeiss Ultra 55) with EDAX (Inca). The functional groups were analysed from FT-IR spectra documented by Perkin-Elmer spectrometer in the range of 400-4000 cm^{-1}. Photoluminescence spectra were taken using a spectrometer JASCO spectro flurometer FP-8200 to study the optical properties.

RESULTS AND DISCUSSION

X-ray diffraction patterns

The X-ray diffraction pattern was obtained in reflection mode with Cu Kα (λ=1.5406 Å) radiation, in the 2Θ range from 10º to 80º at room temperature. Fig. 2 shows the X-ray diffractions patterns of the synthesized of Zn2SnO4 nanoparticles. XRD patterns of synthesized Zn2SnO4 nanorods with diffraction planes (111), (220), (311), (222), (400), (331), (442), (511), (440), (531), (620), (533) and (622), exhibit spinel cubic structure and the values are in a good agreement with the reference JCPDS #74-2184. The lattice constant values a = 8.5814, 8.5871 and 8.5720 Å and volume V = 631.93, 633.19 and 629.86 Å3 for P_1, P_2 and P_3 respectively. The crystallite size of the Zn_2SnO_4 nanorods is measured from Debye Scherrer's relation(eq.1)and the crystallite sizes were found to be 42nm for all the prepared samples (P_1, P_2, and P_3) and the micro-strain (µ) (eq.2) was 0.00082 [16]. In a hydrothermal process, the alkaline concentration is a key factor that influences the crystallinity, morphology, and size of the as-synthesised sample [17]. The XRD pattern indicates that the reaction is complete and the as-synthesised nanorods are close to the expected stoichiometric ratio.

$$D = k\lambda / \beta cos\theta \quad (1)$$

$$\varepsilon = \beta Cos\theta / 4 \quad (2)$$

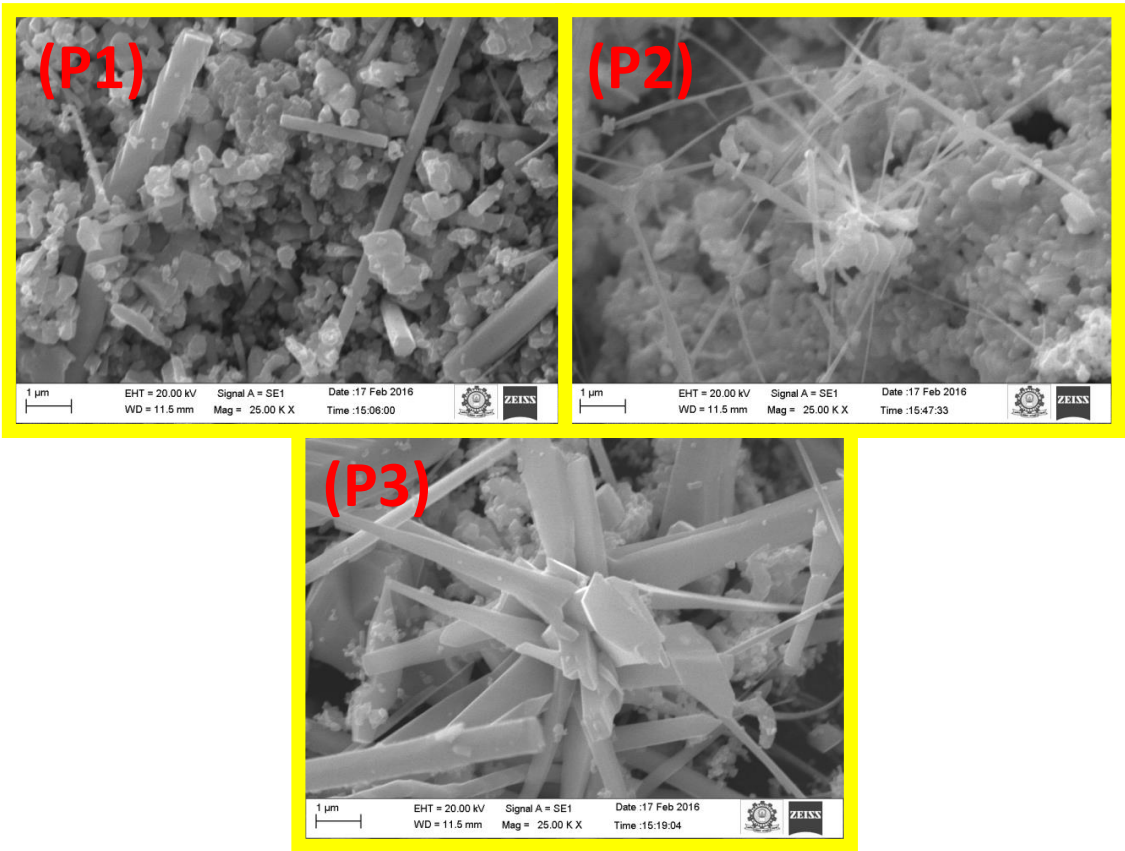

Fig. 3. (P1, P2 and P3) SEM images of Zn_2SnO_4nanorods.

FESEM analysis

The surface morphology of microwave assisted synthesis of all Zn_2SnO_4 nanorods was examined through FESEM analysis was shown in Fig. 3 (P1, P2 and P3). FESEM images clearly showed the synthesized Zn_2SnO_4 exhibits, rod like structure and average particle size in the nanoscale range. The formation of nanorods may be due to two reasons such as crystal nucleation and crystal growth direction. The growth of zinc stannate nanorods is initiated by the reaction between zinc ions and tin ions during hydrothermal synthesis. A part from the reaction time and temperature, the concentration of sodium hydroxide in the precursor solution plays an important role in determining the size and shape of zinc stannate nanoparticles. Zinc hydroxystannate is transformed into zinc stannate at a medium concentration of sodium hydroxide. The growth mechanism of Zn_2SnO_4 nanorods can be explained in terms of chemical reactions and crystal growth, as follows: From the crystallization point of view, the synthesis of an oxide during an aqueous solution reaction is expected to experience a hydrolysis-condensation process. Growth of Zn_2SnO_4 nanorods occurs according to the reaction.

$$Zn(s) \xrightarrow{\Delta} Zn(g)$$

$$Sn(s) \xrightarrow{\Delta} Sn(g)$$

$$2Zn(g) + Sn(g) + 2O_2 = Zn_2SnO_4(s).$$

Elemental compositions analysis

The elemental compositions of the Zn_2SnO_4 nanorods were represented in Fig. 4 (P1, P2 and P3). From the EDAX spectra, the several area positions of the sample were chosen and scanning, the same Zn, Sn and O content was present. In the present work, the Zn, Sn and O elements atomic percentage was given Table 1. The increasing concentration of Tin chloride during synthesis, the oxygen percentage increased and Zinc and tin

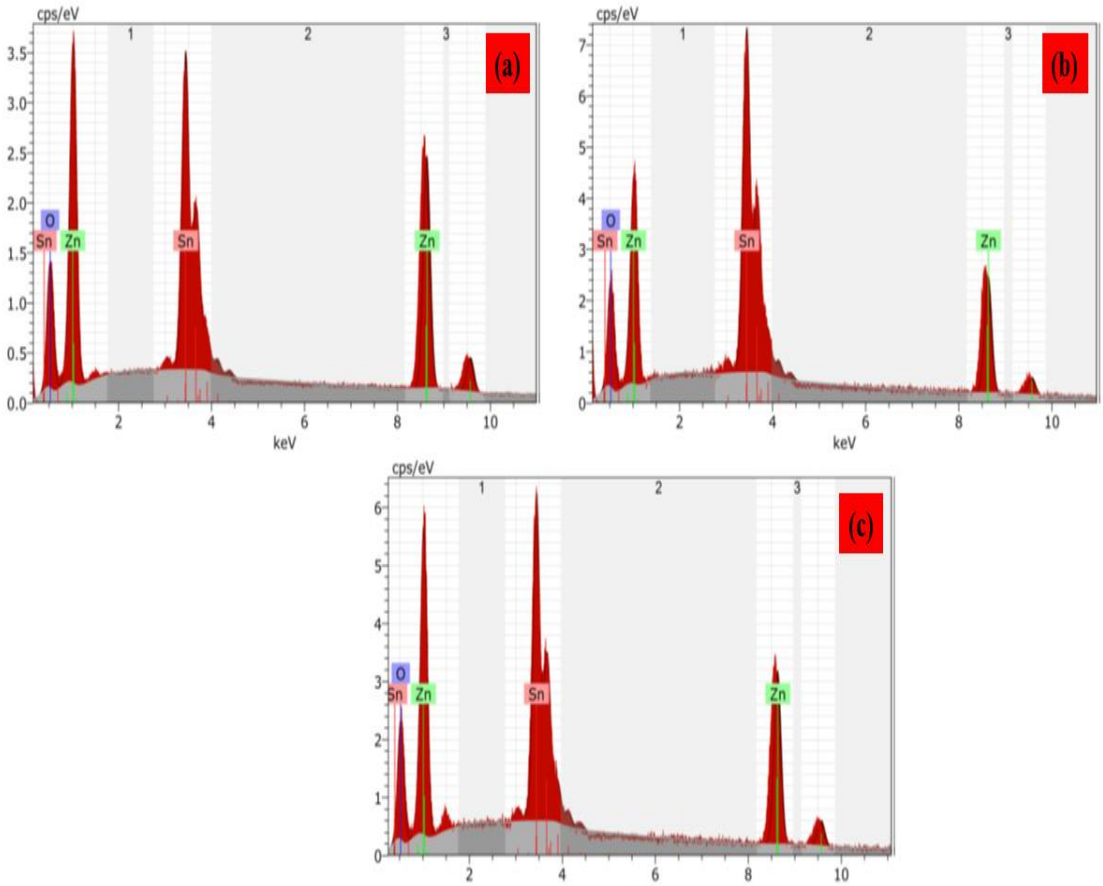

Fig. 4. (a, b and c) EDAX spectra of Zn_2SnO_4 NPs.

Table 1. Elemental composition percentage of Zn_2SnO_4 NPs.

Elements (atomic %)	P1	P2	P3
Tin	13.39	13.53	16.98
Zinc	25.21	24.69	18.26
oxygen	61.40	61.78	64.76

percentage decreased, this may be a local lattice strain.

FTIR spectroscopic analysis

Fig. 5 shows the FTIR spectra of various concentration of Zn_2SnO_4 (2 : 1 (P1), 1 : 1(P2) and 1 : 2 (P3)) NPs. Zn_2SnO_4 samples various functional group are, O-H stretching at (3430, 3432 and 3416 cm^{-1}) [18], C-H stretching at (2921 and 2924 cm^{-1}) [19], C-H bands at (2361 and 2336 cm^{-1}), this can be absorb atmospheric CO_2. The asymmetric and symmetric stretching COO-group was found to be (1620, 1627 and 1632 cm^{-1}) and (1469, 1416 and 1454 cm^{-1}) [19] for P1, P2 and P3 samples. The Zn-Sn-O bands found to be 502, 475 and 460 cm^{-1} for all Zn_2SnO_4 NPs respectively, may be vibration of ZnO and SnO_2 groups, and results formation of the Sn-O-Zn bonding in the Zn_2SnO_4 [20].

Photoluminescence spectroscopic studies

The photoluminescence spectra of microwave assisted Zn_2SnO_4 nanorods was shown in Fig. 6 (P1, P2 and P3).The Zn_2SnO_4 nanorods measured at the excitation wavelength of 460 nm. The two blue-green emission, four green emissions, and orange-yellow emission are located at (484, 499, 508, 519, 526, 541, 555, 566, and 584 nm), (484, 498, 508, 523, 540, 551, 566, and 582 nm) and (484, 499, 509, 519, 526, 541, 555, 566, and 579 nm) for P1, P2 and P3 respectively. The blue-green

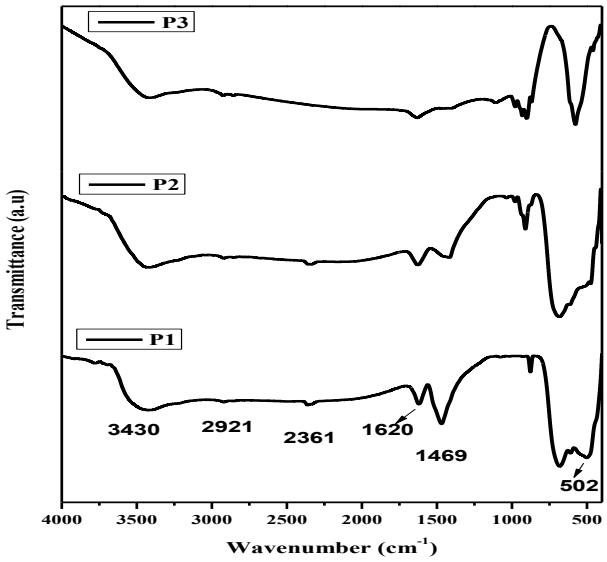

Fig. 5. FTIR spectra of Zn_2SnO_4 NPs (P1, P2, P3).

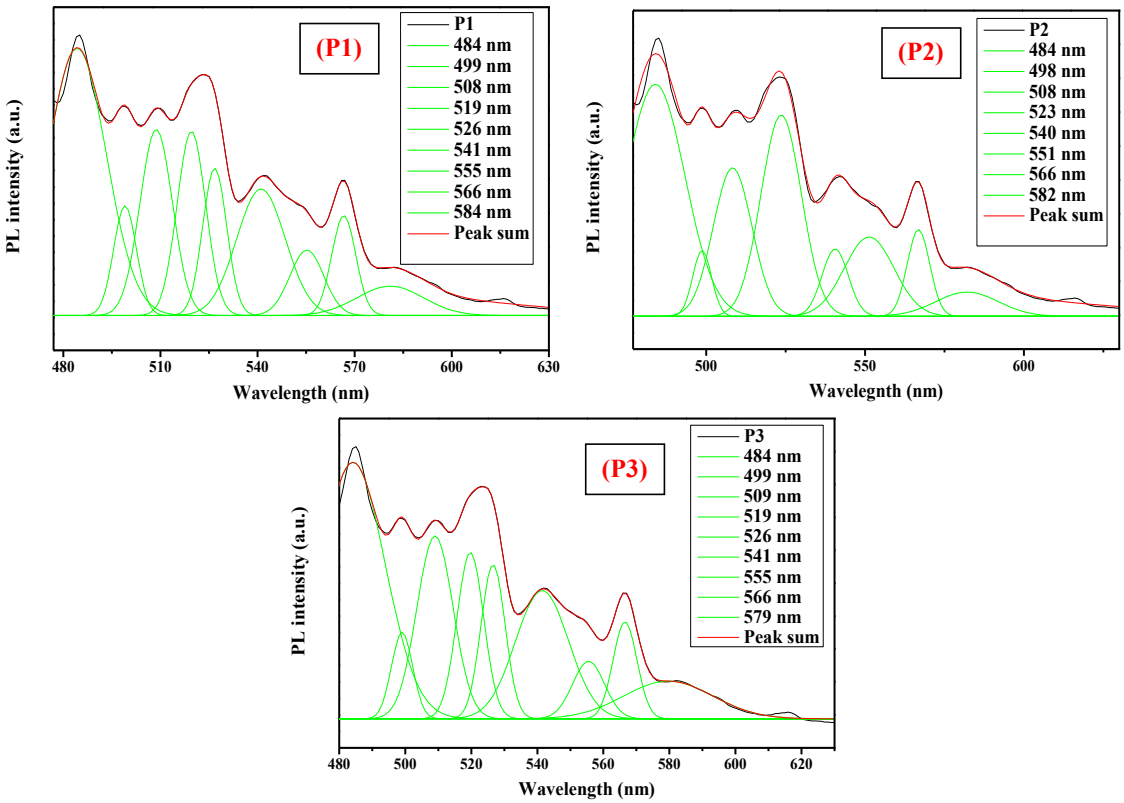

Fig. 6. PL spectra of Zn_2SnO_4 NPs (P1, P2, P3).

emission found to be (484-499 nm) for all Zn_2SnO_4 nanorods, which is attributed to oxygen vacancies [21, 22]. The green emission observed at (508-551 nm) for P1, P2 and P3 samples respectively, usually the oxygen vacancies existing in $ZnSnO_4$ [23, 24]. The yellow-orange emission centered at (566 and 579 nm) for Zn_2SnO_4 nanorods respectively, due to the interaction between

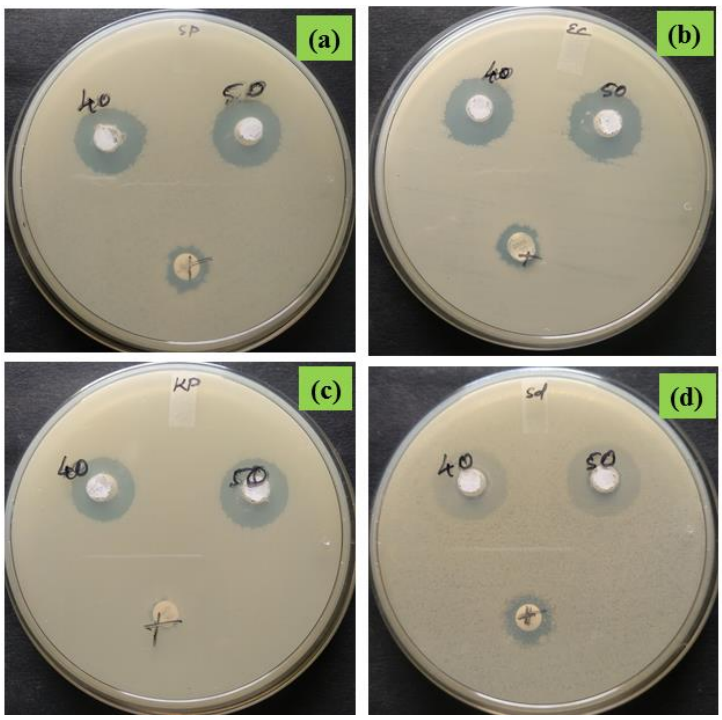

Fig. 7. Progressive antibacterial activity of G+ and G- bacteria (a) *Streptococcus pneumoniae, (b) Escherichia coli,(c) Klebsiella pneumoniae and (d) Shigella dysenteriae*.

oxygen vacancies, tin interstitials and oxygen interstitials can be accountable for the yellow-orange emission [25],and defects has formation of a huge amount of trapped states and sum of meta stable energy levels in the band gap of the as-synthesized Zn_2SnO_4 NPs. However for the P3 sample, green emission values (579 nm) increased as compared to the P2 (582 nm) and P1 (584 nm) for Zn_2SnO_4 nanorods samples respectively. From the optoelectronic application generally depends on decrease in defect level, which is mainly influenced via electron phonon coupling interaction. In the present work, the P3 samples emission decreased as compared to P1 and P2 samples, this results sustenance for the future development of optoelectronic application.

Antibacterial activity

Fig. 7 (P1, P2 and P3) shows antibacterial activity of Microwave assisted Zn_2SnO_4 NPstested against (a) *Streptococcus pneumoniae, (b) Escherichia coli,(c) Klebsiella pneumoniae and (d) Shigella dysenteriae* bacterial strains to determine by the well diffusion method. The Zn_2SnO_4 NPs and Amoxicillin shows the antibacterial activity, which clearly shows the inhibition zone and specifies the biocidal action of Zn_2SnO_4 NPs. The maximum Zone of inhibition was observed *E. coli* as compared to the other *S. pneumoniae, K. pneumoniae and S. dysenteriae bacterial strain* (Fig. 8). In the present work, increasing the concentration (P3) of Zn_2SnO_4 NPs the inhibition zone also gets increased. The mechanism of action Zn_2SnO_4 nanorods is by disruption of bacterial cell membrane by electrostatic interaction leading to bacterial cell death [20].

The size of the inhibition zone increases significantly with the increasing concentration of NPs. Zn_2SnO_4 nanorods have the maximum antibacterial efficacy against *E. coli* with the highest zone of inhibition of 19 mm followed by a zone of inhibition of 18 mm against *S. pneumoniae*. Moderate antibacterial activity against *K. pneumonia* and *S. dysenteriae* with lower zone of inhibition of 12 mm is observed. The toxicity of Zn_2SnO_4 nanorods depends on their concentration and these nanorods are mildly toxic at low concentration. The mechanism of nanoparticle toxicity depends on composition, size, surface modification, intrinsic properties, and bacterial species. Nanorods attach to the bacterial cell membrane by electrostatic interaction and disrupt the integrity of bacterial cell, which in turn increases its permeability leading to cell death.

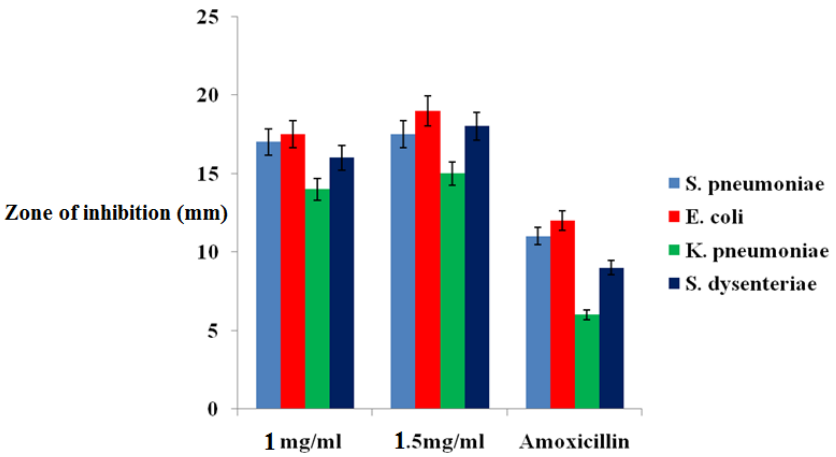

Fig. 8. The Zone of inhibition for various bacterial strain treated with Zn_2SnO_4 NPs.

The toxicity induced due to dissolved Zn ions and Sn ions from Zn_2SnO_4 nanorods is negligible and the toxicity strength of nanorods depends on intrinsic toxic properties of heavy metals [26].

The antibacterial activity generally depends on production of reactive oxygen species (ROS) [27-29].This ROS on the surface of these nanoparticles in light causes oxidative stress in microbial cells membrane, ultimately leading to the death of the cells.

The ROS production using UV light can be given in equation form as the following .

$$Zn_2SnO_4 + h\upsilon \rightarrow e^- + h^+$$

$$h^+ + H_2O \rightarrow {}^{\bullet}OH + H^+$$

$$e^- + O_2 \rightarrow {}^{\bullet}O_2^-$$

$${}^{\bullet}O_2^- + H^+ \rightarrow HO_2^{\bullet}$$

$$HO_2^{\bullet} + H^+ \rightarrow H_2O_2$$

The Zn_2SnO_4 nanorods through defects can be activated via both UV and visible light, electron-hole pairs (e^- h^+) can be created. The holes fragmented H_2O molecules hooked on OH^- and H^+. Dissolved (O_2) can be converted to (${}^{\bullet}O_2^-$) radical anions. The (${}^{\bullet}O_2^-$) superoxide radical anions in turn react with H^+ to create ($HO_2^{\bullet}$) radicals. The hydrogen ions (H^+) react with ($HO_2^{\bullet}$) to produce molecules of H_2O_2. The production of H_2O_2 be able to penetrate the cell membrane and finally bacteria are death [30].On other hand, Zn^{2+}/Sn^{2+}ions are released by Zn_2SnO_4 comes into contact with microbial cell membranes, the cell membranes with (-) charge and Zn^{2+}/Sn^{2+} ions with (+) charge mutually attract. The Zn^{2+}/Sn^{2+} metal ions are penetrates hooked on the cell membrane and react by sulfydryl groups inside the cell membrane. As a result, the damaged microbe synthetase activity and cells losing their ability of cell division, which leads to the cell death of the bacteria.

CONCLUSIONS

In summary, the Zn_2SnO_4 nanorods were prepared through facile hydrothermal method using microwave oven. From the XRD patterns showed that synthesized nanorods exhibits spinel cubic structure. Nanorod like morphology and chemical composition was observed through FESEM and EDAX spectra. In case of FT-IR spectra, the Zn-Sn-O stretching bands was observed at 502, 475 and 460 cm^{-1} for all Zn_2SnO_4 NPs. PL spectra, the Zn_2SnO_4(P3) samples emission decreased as compared to P1 and P2 samples, these results strong support for the potential development of wide-range of optical and electrical device application. The Zn_2SnO_4 nanorods showed the antibacterial activity, the inhibition zone indicates the biocidal action of Zn_2SnO_4 nanorods. This material was used as a bactericidal agent to prevent and control the spread and persistence of infectious diseases.

CONFLICTS OF INTEREST

The authors do not have any personal or financial conflicts of interest.

REFERENCE

1. Ali M. B., Fatiha B. B., Habib E., Brigitte S., Ahmed A., Luc B., Mokhtar F., Rabah B., (2015), Hydrothermal synthesis, phase structure, optical and photocatalytic properties of

Zn_2SnO_4 nanoparticles. *J. Colloid Interface Sci.* 457: 360-369.

2. Zeng J., MuDi X., Kun W. L., Hao W., Hui Y., Wen J. Z., (2008), Transformation process and photocatalytic activities of hydrothermally synthesized Zn_2SnO_4 nanocrystals. *J. Phys. Chem.* 112: 4159-4167.
3. Wang W-W., Zhu Y-J., Yang L-X., (2007), ZnO–SnO_2 hollow spheres and hierarchical nanosheets: hydrothermal preparation, formation mechanism, and photocatalytic properties. *Adv. Funct. Mater.* 17: 59-64.
4. Fu G., Huan C., Zhexiong C., Jinxiu Z., Heinz K., (2002), Humidity sensitive characteristics of Zn_2SnO_4–$LiZnVO_4$ thick films prepared by the sol–gel method. *Sens. Actuators B Chem.* 81: 308-312.
5. Šepelák V., Sebastian M. B., Ingo B., Sylvio I., Marco S., Armin F., Christian K., (2012), Nonequilibrium structure of Zn_2SnO_4 spinel nanoparticles. *J. Mater. Chem.* 22: 3117-3126.
6. Jaculine M., Justin Raj C., Jerome Das S., (2013), Hydrothermal synthesis of highly crystalline Zn_2SnO_4 nanoflowers and their optical properties. *J. Alloys Compd.* 577: 131-137.
7. ZhaoY., Ying H., Qiufen W., Ke W., Meng Z., Lei W., Wei Z., Xu S., (2013), Preparation of hollow Zn_2SnO_4 boxes for advanced lithium-ion batteries. *RSC Adv.* 3: 14480-14485.
8. Raja A., Ashokkumar S., Pavithra Marthandam R., Jayachandiran J., Chandra Prasad K., Kaviyarasu K., Ganapathi Raman R., Swaminathan M., (2018), Eco-friendly preparation of zinc oxide nanoparticles using *Tabernaemontana divaricata* and its photocatalytic and antimicrobial activity. *J Phochem. Photobio. B*. 181: 53-58.
9. Dinesh S., Barathan S., Premkumar V. K., Sivakumar G., Anandan N., (2016), Hydrothermal synthesis of zinc stannate (Zn_2SnO_4) nanoparticles and its application towards photocatalytic and antibacterial activity. *J. Mater. Sci.: Mater. Electron.* 27: 9668-9675.
10. Abdulrahman H., Chandrasekaran K., Abdulazees Parveez A., Nooruddin T., Naiyf S. A., Sulaiman Ali A., Ganasan R., (2016), In vitro antibacterial activity of ZnO and Nd doped ZnO nanoparticles against ESBL producing Escherichia coli and Klebsiella pneumoniae. *Sci. Rep.* 6: 24312-24318.
11. Foster H., Iram B. D., Sajnu V., Alex S., (2011), Photocatalytic disinfection using titanium dioxide: Spectrum and mechanism of antimicrobial activity. *Appl. Microbiol. Biotechnol.* 90: 1847-1868.
12. Samreen F., Mahendra S., Mazahar F., Pathan M., (2019), Biosynthesis of Silver nanoparticle using aqueous extract of Saraca asoca leaves, its characterization and antimicrobial activity. *Int. J. Nano Dimens.*10: 163-168.
13. Leila K., Robabe M., Shahin K., (2018), Influence of reaction parameters on crystal phase growth and optical properties of ultrasonic assisted Hydro-and solvothermal synthesized sub-micrometer-sized CdS spheres. *Int. J. Nano Dimens.* 9: 346-356.
14. Assi N., Abroumand Azar P., Saber Tehrani M., Husain S. W., Darvish M., Pourmand S., (2017), Synthesis of ZnO-nanoparticles by microwave assisted sol-gel method and its role in photocatalytic degradation of food dye Tartrazine. *Int. J. Nano Dimens.* 8: 241-249.
15. Rejani P., Asha R., Beena B., (2014), Structural, optical and dielectric studies in ZnO nanorods by microwave assisted method. *Int. J. Nano Dimens.* 5: 497-503.
16. Hankare P. P., Chate P. A., Sathe D. J., Chavan P. A., Bhuse V. M., (2009), Effect of thermal annealing on properties of zinc selenide thin films deposited by chemical bath deposition. *J. Mater. Sci.: Mater. Electron.* 20: 374-379.
17. Sepelák V., Becker S. M., Bergmann I., Indris S., Scheuermann M., Feldhoff A., Kübel C., Bruns M., Stürzl N., Ulrich A. S., Ghafari M., Hahn H., Grey C. P., Beckerbk K. D., Heitjans P., (2012), Nonequilibrium structure of Zn_2SnO_4 spinel nanoparticles. *J. Mater. Chem.* 22: 3117–3126.
18. Wang Y., Liao X., Huang Z., Yin G., Gu J., Yao Y., (2010), *X*-ray diffractometer patterns of the pure and Cedoped ZnO nanostructures exhibit hexagonal wurtzite crystal structure. *Colloids Surf.* A. 372: 165-172.
19. Vijayaprasath G., Soundarrajan P., Ravi G., (2018), The point defects induced ferromagnetism in ZnO semiconductor by terbium doping via co-precipitation method. *J. Mater. Sci.: Mater. Electron*. 29: 11892-11900.
20. Jeronsia J., Allwin Joseph L., Mary Jaculine M., Annie Vinosha P., Jerome Das S., (2016), Hydrothermal synthesis of zinc stannate nanoparticles for antibacterial applications. *J. Taibah. Univ. Sci.* 10: 601-606.
21. Wang J. X., Xie S. S., Gao Y., Yan X. Q., Liu D. F., Yuan H. J., Zhou Z. P., (2004), Growth and characterization of axially periodic Zn_2SnO_4 (ZTO) nanostructures. *J. Cryst. Growth.* 267: 177-183.
22. Wang J. X., Xie S. S., Yuan H. J., Yan, X. Q., Liu D. F., Yuan H. J., Zhou Z. P., (2004), Synthesis, structure, and photoluminescence of Zn_2SnO_4 single-crystal nanobelts and nanorings. *Solid State Commun.* 131: 435-440.
23. Wang J., Xiao W. S., Shishen X., Weiya Z., Yi Y., (2007), Single-crystal and twinned Zn_2SnO_4 nanowires with axial periodical structures. *Cryst. Growth Des.* 8: 707-710.
24. Kim H. S., Seon O. H., Yoon M., Jeunghee P., Seung Y. B., Jae P. A., (2008), Three-dimensional structure of helical and zigzagged nanowires using electron tomography. *Nano Let.* 8: 551-557.
25. Applerot G., Lellouche J., Perkas N., Nitzan Y., Gedanken A., Banin E., (2012), ZnO nanoparticle-coated surfacesinhibit bacterial biofilm formation and increase antibiotic susceptibility. *RSC Adv.* 2: 2314–2321.
26. Zhao J-W., Li-Rong Q., Zhang L-D., (2007), Single-crystalline Zn_2SnO_4 hexangular microprisms: Fabrication, characterization and optical properties. *Solid state commun.* 141: 663-666.
27. Li Q., Shaily M., Delina Y. L., Lena B., Michael V. L., Dong L., Pedro J. A., (2011), Antimicrobial nanomaterials for water disinfection and microbial control: Potential applications and implications. *Water Res.* 42: 4591-4602.
28. Foster H. A., Iram B. D., Sajnu V., Alex S., (2011), Photocatalytic disinfection using titanium dioxide: Spectrum and mechanism of antimicrobial activity. *Appl. Microbiol. Biotechnol.* 90: 1847-1868.
29. Wilson M. R., Janet H. L., Ken D., Jill S., Vicki S., (2002), Interactions between ultrafine particles and transition metals in vivo and in vitro. *Toxicol. Appl. Pharm.* 184: 172-179.
30. Fang M., Chen J-H., Xu X-L., Yang P-H., Hartmut F. H., (2006), Antibacterial activities of inorganic agents on six bacteria associated with oral infections by two susceptibility tests. *Int. J. Antimicrob. Agents.* 27: 513-517.